Biochemical and Biophysical Research Communications 441 (2013) 782–786

Contents lists available at ScienceDirect

Biochemical and Biophysical Research Communications

journal homepage: www.elsevier.com/locate/ybbrc

Characterization of a dwarf mutant allele of *Arabidopsis* MDR-like ABC transporter *AtPGP1* gene

Lingfeng Ye [a], Lin Liu [a], Anqi Xing [b], Dingming Kang [a,*]

[a] College of Agronomy and Biotechnology, Beijing Key Laboratory of Crop Genetic Improvement, China Agricultural University, Beijing 100193, China
[b] National Maize Improvement Center of China, China Agricultural University, Beijing 100193, China

ARTICLE INFO

Article history:
Received 23 October 2013
Available online 5 November 2013

Keywords:
Polar auxin transport (PAT)
Dwarf
Mutant
Arabidopsis thaliana

ABSTRACT

Asymmetric auxin distribution caused by polar auxin transport (PAT) regulates many plant developmental and physiological processes. Plant two closely ABC (ATP-binding cassette) transporter, AtPGP1 and AtPGP19 (AtMDR1), have been implicated in auxin transport. However, unlike *atpgp19* mutant and *atpgp1 atmdr1* double mutant show decreased apical dominance, reduced growth, and impaired basipetal auxin transport, *atpgp1* mutant exhibit no significant difference from wild type. We report a new allele of *atpgp1* mutants, designated as *atpgp1-2*, which showed shorter hypocotyl and dwarf phenotype under long-day condition. Auxin transport activity was greatly impaired and NPA-sensitivity was decreased in the mutant. Moreover, we detected transcript in the *atpgp1* mutants reported previously, but not in *atpgp1-2*. These results suggest a direct involvement of AtPGP1 in auxin transport processes controlling plant growth.

1. Introduction

Auxin (typically indole-3-acetic acid; IAA) is known to be involved in diverse roles in the regulation of plant growth and development, such as embryogenesis, organ development, tropism and other developmental and physiological processes [1,2]. Auxin gradients caused by polar auxin transport (PAT) provide the directional information required for the coordination of plant development [3]. PAT is described by a chemiosmotic model in which cellular influx and efflux of auxin is mediated by both membrane diffusion and carrier-mediated transport [4,5]. Several classes of auxin transporter proteins have been identified through molecular genetic studies in *Arabidopsis thaliana* for the past decade. The direction of auxin flow is determined by the polar plasma membrane localization of these carriers. AUX RESISTANT 1/LIKE AUX1 (AUX1/LAX) transmembrane proteins were seemed to be involved in the influx of IAA; the agravitropic phenotype aux1 mutant is deficient in basipetal auxin transport [6,7]. PIN-FORMED (PIN) proteins show polar distributions on cell membranes and are involved in some aspect of auxin efflux. In *Arabidopsis*, eight *PIN* genes have been reported [8–10]. The phenotypes of *pin* mutants can be phenocopied by treatment with auxin efflux inhibitors, such as 1-naphthylphthalamic acid (NPA) [11].

P-GLYCOPROTEIN/MULTIDRUG RESISTANCE (PGP/MDR) proteins are the member of ATP-binding cassette (ABC) protein superfamily. PGP proteins have two similar halves contained a transmembrane domain (TMD) and a nucleotide-binding domain (NBD) in the predicted protein [12,13]. In *Arabidopsis*, 22 *PGP* genes (21 transcribed genes, 1 pseudogene) have been identified and were divided into three clusters [14,15]. Some proteins function in auxin efflux and some in auxin influx [16]. As with the functional mechanism of PGPs, one of its working models indicated that PGPs probably interact with other regulatory proteins, such as the immunophilin-like TWISTED DWARF 1 (TWD1) and PIN, regulate auxin transport activity [17,18], but also PGPs may mediate direct auxin transport [19].

AtPGP1 and its closest homolog, AtMDR1 (AtPGP19), have been shown to be involved in polar auxin transport. AtPGP1 exhibited polar plasma membrane localization in elongating and matured tissues, but non-polar localization at the shoot and root apices [19]. Over-expression of *AtPGP1* resulted in longer hypocotyls in *Arabidopsis* grown under dim light [20]. In a subsequent study, *atmdr1* and *atpgp1 atmdr1* double mutant, but not *atpgp1*, conferred dwarfism and epinastic cotyledons; polar auxin transport was found impaired in both *atmdr1* single mutant and *atpgp1/atmdr1* double mutant with the double mutant having a more severe reduction [21]. In addition, both *atpgp1* and *armdr1* mutants were insensitive to NPA, suggesting their roles in mediating polar auxin transport [21,22]. Moreover, expression of *AtPGP1* in yeast

* Corresponding author. Fax: +86 10 62732568.
E-mail address: kdm@pku.edu.cn (D. Kang).

0006-291X
http://dx.doi.org/10.1016/j.bbrc.2013.10.136

and mammalian cells enhanced efflux of indole-3-acetic acid (IAA) and the synthetic auxin 1-naphthalene acetic acid (1-NAA) [17,19]. The *PGP1* ortholog has been cloned in maize (*Brachytic2/ZmPGP1*) and in Sorghum (*Dwarf3/SbPGP1*) and the mutants shown reduced basipetal auxin transport and compact lower stalk internodes [23,24].

Here, we report that a new allele of *atpgp1* mutants, which showed shorter hypocotyls and dwarf phenotypes, distinguished with the reported mutants under long-day condition. The mutant exhibited reduced IAA transport and exhibit decreased NPA-sensitivity. We compared the mutated site with another two allele mutants reported previously and detected the variant length transcript. We demonstrated that *atpgp1* mutant is a new allele and null mutant of *AtPGP1*.

2. Materials and methods

2.1. Isolation of atpgp1 mutant

The *Arabidopsis thaliana* mutant SAIL_716_H02, designated *atpgp1-2*(At2g36910), was obtained from ABRC (Ohio State University, Columbus, OH). The wild-type and mutant ecotype both are Col-0. The homozygous lines were confirmed by PCR with the primer 716F: GAAGAGCCTAAGAAAGCAGA, 716R: GGTCAAA TGGTGGCGAACTA and LB2: GCTTCCTATTATATCTTCCCAAATTACC AATACA, followed standard procedure http://signal.salk.edu/tdnaprimers.2.html. The T-DNA insertion sites were confirmed by PCR with the primer 716R/ LB2 and sequencing. For the *atpgp1-100* (SALK_083649C), *atpgp1-101* (SALK_046440) and *atmdr1* (SALK_033455) mutants, we used PCR genotyping to verify homozygous lines as described by Lin and Wang [25].

2.2. Semi-quantitative RT-PCR

Plant total RNA was extracted from 7-days seedlings using Trizol reagent (Invitrogen) and was reverse transcribed using Reverse Transcriptase M-MLV (Takara) according to the manufacturer's protocol. Primers for the RT-PCR were ActinF: CATCAGGAAGG ACTTGTACGG, ActinR: GATGGACCTGACTCGTCATAC for actin control, P1: CGCCGACGGATTAGATTATG, P8: TCAGAGACACTTCCTTGC and P10: TGGAGAAGTCAGAGATGCCG for *AtPGP1*.

2.3. Plant growth conditions

Seeds were sterilized with 1% sodium hypochlorite solution plus 0.01% (v/v) Triton X-100 for 5 min and washed 7 times with sterile water. Sterilized seeds were then sown on plates with 1/2 MS agar medium (2.2 g/L Murashige and Skoog basal medium [Sigma–Aldrich], 1% [w/v] sucrose and 0.8% [w/v] agar, pH 5.8) and maintained for 2–3 day at 4 °C. Seedlings were grown under long day condition: 16 h photoperiod with 100 μmol m^{-2} s^{-1} white light at 22 °C.

2.4. Plant hypocotyl and silique length, height measurement

Arabidopsis seedlings of 7 days were spread on 1/2 MS agar medium and pictures were taken with digital camera (Nikon D7000, Tokyo). Hypocotyl and silique length was measured by ImageJ software (National Institutes of Health, http://imagej.nih.gov/ij). Plant height of 28-days old was measured with a ruler which has one scale in centimeters.

2.5. Scanning electron microscopy of hypocotyl cells

For scanning electron microscopy, seedlings were fixed for 4 h at 4 °C in FAA solution containing 5% formaldehyde, 5% acetic acid, and 63% ethanol. Fixed samples were dehydrated in 100% ethanol, critical point drying (HITACHI, HCP-2), and coating with Pt (Eiko IB.3, ION COATER). Scanning electron microscope (HITACHI S-3400N) was used for imaging.

2.6. Histochemical GUS staining

For histochemical GUS staining, 5 days grown seedlings were incubated in a solution containing 50 mM sodium phosphate buffer, 2 mM $K_3Fe(CN)_6$, 2 mM $K_4Fe(CN)_6$, 10 mM EDTA, 0.1% Triton X-100 (v/v), and X-glu at 37 °C for 8 h and examined under a microscope.

2.7. Polar auxin transport measurements

Auxin transport assays of light-grown seedlings were performed according to the method described previously [26], with some modifications. Primary inflorescence were grown for 28–30 days with the 10–15 cm stems length, segments of 2.5 cm were excised that spanned from 5 to 7.5 cm above the base of the inflorescence. Segments with apical end submerged in 30 μl of 1/2MS agar medium that contained 0.35% phytogel, 500 nM unlabelled IAA (sigma–Aldrich) and 500 nM [^{3}H]IAA (specific activity 20 Ci $mmol^{-1}$, American Radiochemical, St. Louis, MO) with or without 15 μM NPA. The segments incubated for 4 h at 25 °C. After incubation, a 5 mm section from the basal end of segment was excised and washed twice with 1/2 MS liquid medium. The segments were then incubated in 1 ml scintillation fluid for 16 h and counted by scintillation counter (Perkin-Elmer MicroBetaTriLux1450).

3. Results

3.1. Isolation of atpgp1 mutant alleles

Three separate populations of T-DNA insertion lines of *AtPGP1* gene, SAIL_716_H02, SALK_083649 and SALK_046440 (renamed as *atpgp1-2*, *atpgp1-100* and *atpgp1-101*, respectively) from Salk Institute was screened by PCR, as described by Krysan et al [27]. The homozygous mutant lines of T-DNA insertion were collected. Sequencing analysis indicated that the *atpgp1-2* contained a T-

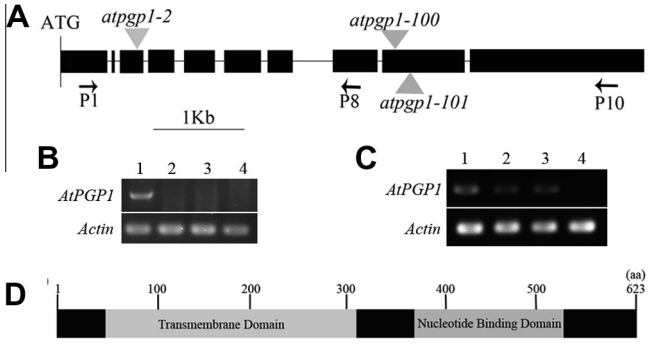

Fig. 1. *atpgp1* mutant identification. (A) Genomic structure of *AtPGP1* and T-DNA insertion positions. Black rectangles represent the exons, and lines represent introns. Triangles represent T-DNA insertions. Arrowheads indicates primers used to screen for the mutants. (B) RT-PCR analysis of the *atpgp1* mutant used primers P1 and P10. Lane 1, wild type (Col); Lane 2, *atpgp1-100*; Lane 3, *atpgp1-101;* Lane 4, *atpgp1-2*. (C) RT-PCR analysis of the *atpgp1* mutant used primers P1 and P8. Lane 1, wild type (Col); Lane 2, *atpgp1-100*; Lane 3, *atpgp1-101;* Lane 4, *atpgp1-2*. (D) The conserved domains translated by the first exon to the eighth exon of *AtPGP1* gene.

DNA insertion in the third exon, both *atpgp1-100* and *atpgp1-101* contained a T-DNA insertion in the ninth exon but at different locations (Fig. 1A).

To determine the expression of AtPGP1 in three mutants, total RNA were isolated from seedlings of mutants and wild type. RT-PCR showed no *AtPGP1* mRNA detected in all three mutants seedlings when use the P1 and P10 primers (Fig. 1B). However, RT-PCR detected transcript in *atpgp1-100* and *atpgp1-101* mutants using the P1 and P8 primers (Fig. 1C). As showed (Fig. 1D), *atpgp1-100* and *atpgp1-101* mutants probably translated truncated protein containing ABC transporter transmembrane region (TMD, aa 49-316) and nucleotide binding domain (NBD, aa 386-535).

3.2. Phenotypic characterization of atpgp1-2

Both *atpgp1-100* and *atpgp1-101* were previously reported to have no obvious phenotype difference from their wild type plants [21,25], our results also indicate no significant difference in plant morphology at both seedling and adult stages compared to that of the wild type plants (Data not shown).

In order to characterize the phenotypic effect caused by the T-DNA insertion in *atpgp1-2*, the mutant and wild type plants were grown under both dark and light conditions. Seedlings were harvested 7 days after emergence. Hypocotyl length was measured and submitted to significant test. Dark-grown *atpgp1-2* and wild type plants exhibit no significant difference in hypocotyl length, while significant difference was detected between light grown *atpgp1-2* and wild type plants (Fig. 2A and B). Microscopic examination further revealed that *atpgp1-2* mutant has shorter epidermal cells which underlies the shortening of light grown hypocotyls.We measure the plant height of 4-week-old *atpgp1-2* mutant under long-day condition (16 h light/8 h dark). A dwarf phenotype in plant height in *atpgp1-2* mutant is observed, statistical date revealed that plant height of *atpgp1-2* was reduced by 24.5% compared to that of wild type plants (Fig. 2E, Table 1), in addition, silique size of *atpgp1-2* is also reduced much compared with wild type plants (Fig. 2F).

3.3. atpgp1-2 shows reduced IAA accumulate in root apex

To detect the IAA accumulate levels of *atpgp1-2* mutant, *ProDR5:GUS* auxin response reporter was crossed into *atpgp1-2* seedlings, the expression of GUS were visualized in wild-type and mutant root apices by microscopy. Expression of GUS was

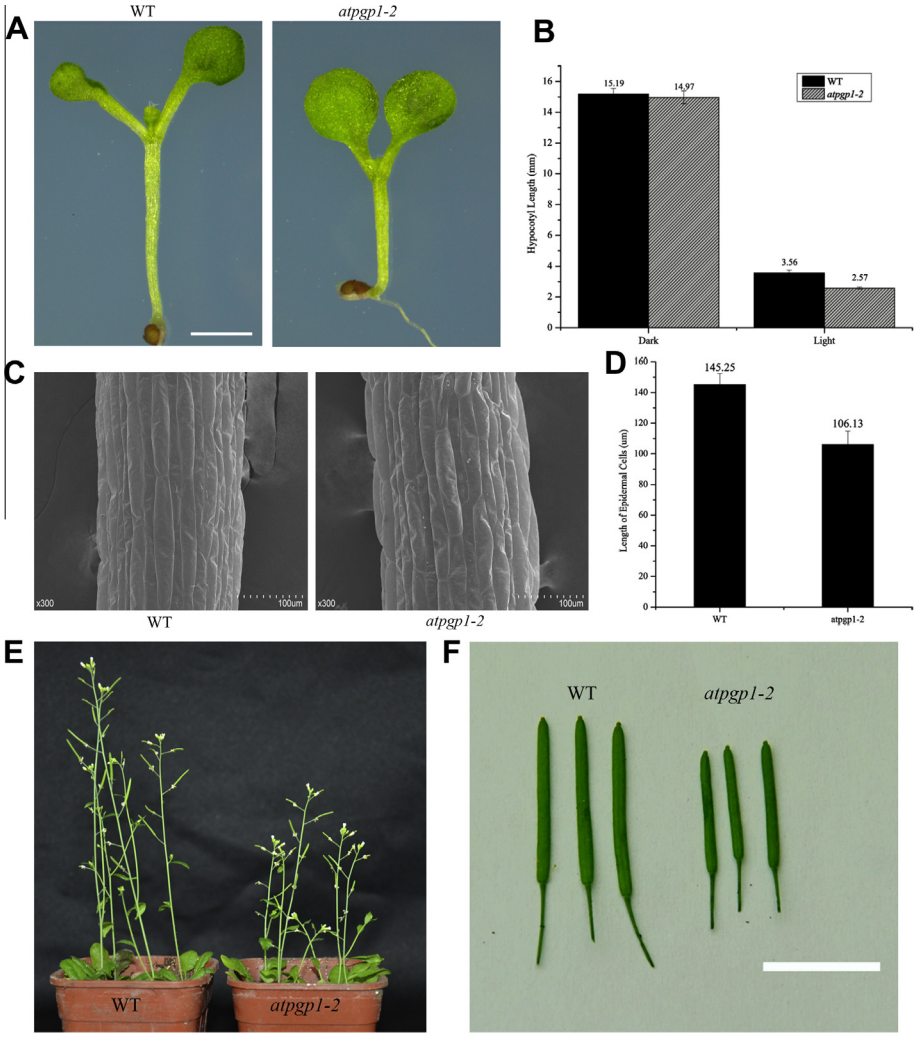

Fig. 2. Morphology of *atpgp1-2*. (A) *atpgp1-2* (right) showed shorter hypocotyl compared with wild type (left) under long-day conditions grown for 7 days. Bar indicates 1 mm. (B) Hypocotyl lengths of *atpgp1-2* and wild type. Seedlings were grown in darkness and long-day conditions for 7 days. Each data point represents the average length of 20 seedlings. Error bars indicate ± SD. Bar indicates 100 μm. (C) Scanning electron microscopy of hypocotyls of wild type (left) and *atpgp1-2* (right). (D) Epidermal cell length of wild type and *atpgp1-2*. Error bars indicate ± SD. (E) *atpgp1-2* showed dwarf phenotype under long-day conditions grown for 28 days. (F) *atpgp1-2* had smaller siliques. Bar indicates 1 cm.

Table 1
Plant height and silique length of *atpgp1-2* mutant and wild type.

Line	Plant height (cm)	Silique length (mm)
WT	14.54 ± 0.49	15.79 ± 1.7
atpgp1-2	10.974 ± 0.58**	11.12 ± 1.23**

** Significantly different from WT ($P < 0.01$). For plant height, $n = 20$; for silique length, $n = 15$.

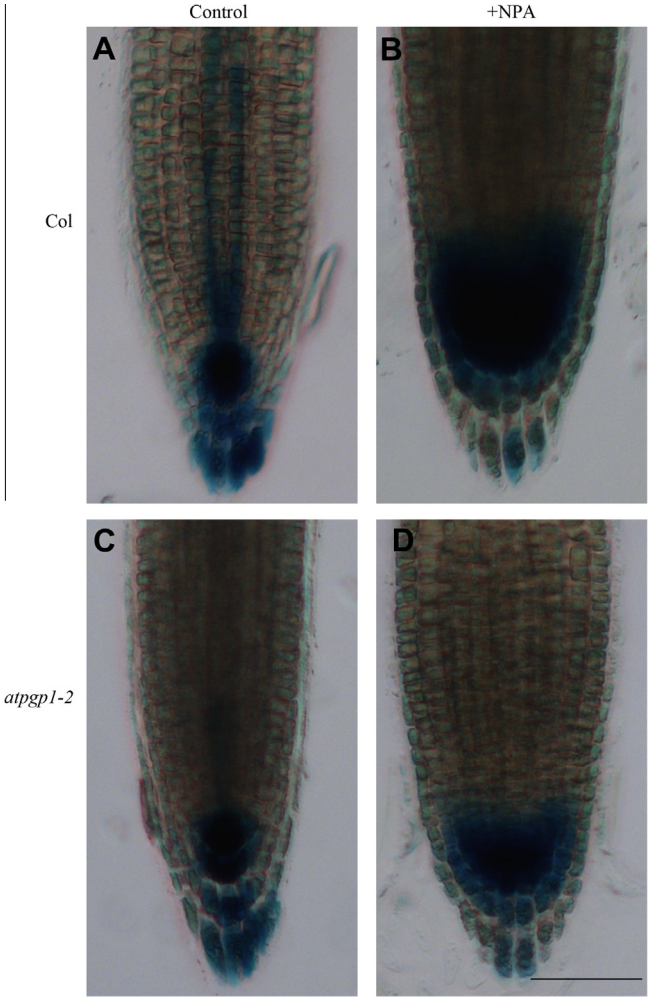

Fig. 3. *Pro$_{DR5}$:GUS* expression in 5-day seeding root tips. (A) GUS staining pattern in root tips of wild type (Col). (B) GUS staining pattern in wild type root tips after treatment with 5 μM NPA for 2 days. (C) GUS staining pattern in root tips of *atpgp1-2*. (D) GUS staining pattern in *atpgp1-2* root tips after treatment with 5 μM NPA for 2 days. Bar indicates 100 μm.

reduced in *atpgp1-2* compared with wild type (Fig. 3A and C). This revealed lesser accumulation of auxin in the *atpgp1-2* root tips, suggested PGP1 mediated basipetal transport in root apices. Auxin efflux inhibitor 1-*N*-naphthylphthalamic acid (NPA) treatment significantly caused an relatively more increased expression of *ProDR5:GUS* in wild type root tip than do *atpgp1-2* mutant (Fig. 3B and D). This result suggests that the *atpgp1-2* mutant is less sensitive to NPA inhibition of auxin transport and accumulate relatively less auxin in the root tips than do wild-type plants.

3.4. Polar auxin transport is reduced in atpgp1-2

Measurements of basipetal transport of [^{3}H]IAA in light-grown 7 days hypocotyls of *atpgp1-2*, *atmdr1* (*atpgp19*) mutants and wild

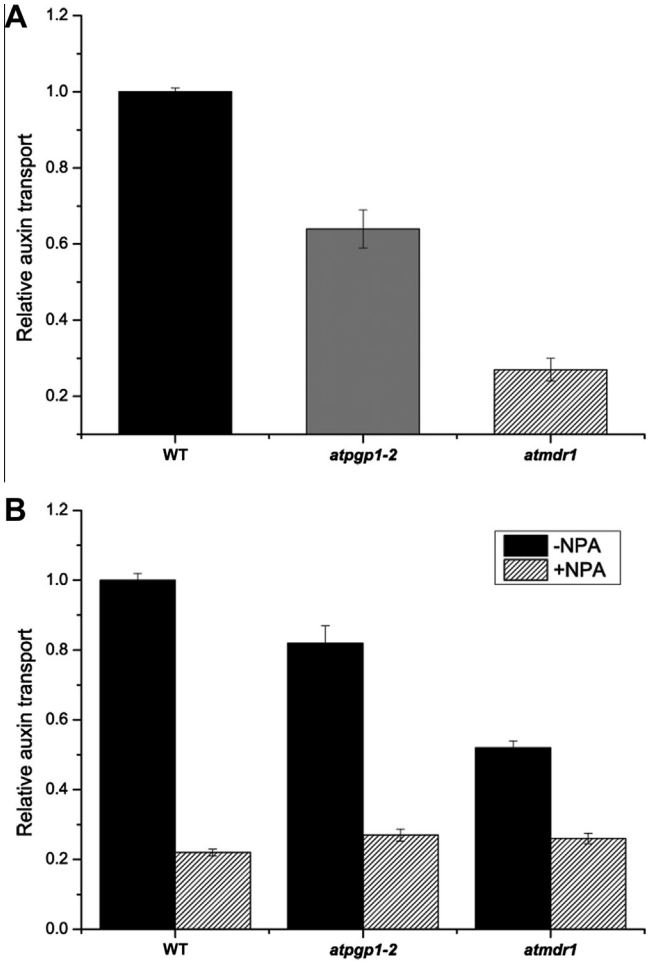

Fig. 4. Transport of [^{3}H]IAA in the mutants and wild type. (A) Relative auxin transport activity in hypocotyls of 7-days seedlings. Each assay used 10 seedings. Error bars indicate ± SD. (B) Relative auxin transport activity in apical sections of inflorescence stems. Each assay used 8 plants. Error bars indicate ± SD.

type showed a great reduction in both *atpgp1-2* and *atmdr1*, but more drastic in *atmdr1* (Fig. 4A).The polar auxin transport of excised segments of the 27 days upper inflorescence stems were measured according to the protocol described with some modifications, as shown in Fig. 4B, only slight difference were seen between *atpgp1-2* and wild type, but *atmdr1* were clearly defective in polar auxin transport. We also examined the sensitivity of PGP-mediated auxin transport to the auxin efflux inhibitor NPA, the auxin efflux were blocked in the mutants and wild type. However, the wild type showed more reduction compared to *atpgp1-2* and *atmdr1* in inflorescence stems.

4. Discussion

The *Arabidopsis* ABCB1 and ABCB19 proteins have been extensively characterized and a lot of physiological, cellular, and biochemical data confirmed their function as auxin-transport carriers. Unlike *atpgp19* and *atpgp1*/*atpgp19* double mutants show reduced growth, curled rosette leaves, and impaired basipetal auxin transport [21]. However, *atpgp1* mutants show no morphological differences from wild type at seedling or adult stage. In this paper, we identified a new *atpgp1* mutant, designated as *atpgp1-2*, which has a T-DNA insertion in the third exon. We substantiated that *atpgp1-2* was a new allele mutant distinguished from another two *atpgp1* mutants named *atpgp1-100* and *atpgp1-101*[21,25]. It

showed reduced hypocotyls growth and dwarfism at adult stage under long-day conditions, which is different from previous reported allele mutants of *AtPGP1*. Further, *atpgp1-2* exhibited significantly reduced both in expression of the auxin responsive *DR5*::*GUS* reporter gene and in the polar auxin transport. These results give the compelling evidence that *AtPGP1* function in auxin transport, loss of *AtPGP1* can also exhibit noticeable auxin-related phenotypes.

Since *atpgp1-100* and *atpgp1-101* both have a T-DNA insertion in the ninth exon and show no obvious phenotype difference from wild type, we designed a series of reverse primers at each exon of *AtPGP1*, expression analysis by the RT-PCR detected transcript in *atpgp1-100* and *atpgp1-101*, but not in *atpgp1-2*. Thus, it is speculated that *atpgp1-2* could be a null mutant allele, but *atpgp1-100* and *atpgp1-101* probably are not, and more, *atpgp1-100* and *atpgp1-101* mutants probably encode truncated proteins of ~600 amino acids containing one TMD and one NBD. On the other hand, we transformed *atpgp1-2* mutant with a construct containing the 35S promoter driving the *ZmPGP1* complementary DNA, this construct was capable of rescued the hypocotyls length and plant height defect (Our unpublished data). These results are consistent with a role of PGP1 in functional auxin efflux transporter.

Moreover, these results suggest that the different site mutations of *PGP1* gene may result in different phenotype and basipetal auxin flux. We identified a SNP variant mutant allele of maize *Brachytic2*/*ZmPGP1*, which showed mild decreased plant height and mild impairment in auxin movement, seems to corroborate this hypothesis (Our unpublished data). Therefore, it is implicated that some genetic variants of the *PGP1* homologous genes in other crops could be screened for discovering a mild regulation of plant height development applied in crops improvement.

Acknowledgment

We thank Dr. Lijia Qu for conmments the manuscript and Dr. Genji Qin for help in the pictures. This work was supported by National Nature Foundation of China (31171564) and Transformation Science and Technology Program of China (2013ZX08010001-009).

References

[1] R. Benjamins, B. Scheres, Auxin: the looping star in plant development, Annu. Rev. Plant Biol. 59 (2008) 443–465.
[2] O. Leyser, The power of auxin in plants, Plant Physiol. 154 (2010) 501–505.
[3] C. Forestan, S. Varotto, The role of PIN auxin efflux carriers in polar auxin transport and accumulation and their effect on shaping maize development, Mol Plant 5 (2012) 787–798.
[4] P.H. Rubery, A.R. Sheldrake, Carrier-mediated auxin transport, Planta 118 (1974) 101–121.
[5] J.A. Raven, Transport of indoleacetic acid in plant cells in relation to pH and electrical potential gradients, and its significance for polar IAA transport, New Phytol. (1975) 163–172.
[6] R. Swarup, J. Kargul, A. Marchant, Structure–function analysis of the presumptive *Arabidopsis* auxin permease AUX1, Plant Cell 16 (2004) 3069–3083.
[7] Y. Ugartechea-Chirino, R. Swarup, K. Swarup, et al., The AUX1 LAX family of auxin influx carriers is required for the establishment of embryonic root cell organization in *Arabidopsis thaliana*, Ann Bot (Lond) 105 (2010) 277–289.
[8] K. Zažímalová, P. Křeček, P. Skůpa, et al., Polar transport of the plant hormone auxin – the role of PIN-FORMED (PIN) proteins, Cell. Mol. Life Sci. 64 (2007) 1621–1637.
[9] J. Friml, Subcellular trafficking of PIN auxin efflux carriers in auxin transport, Eur. J. Cell Biol. 89 (2010) 231–235.
[10] Z. Ding, B. Wang, I. Moreno, et al., ER-localized auxin transporter PIN8 regulates auxin homeostasis and male gametophyte development in *Arabidopsis*, Nature 3 (2012) 1–9.
[11] H. Tanaka, P. Dhonukshe, P.B. Brewer, et al., Spatiotemporal asymmetric auxin distribution: a means to coordinate plant development, Cell. Mol. Life Sci. 63 (2006) 2738–2754.
[12] R. Sánchez-Fernández, T.G.E. Davies, J.O.D. Coleman, et al., The *Arabidopsis thaliana* ABC protein superfamily, a complete inventory, J. Biol. Chem. 276 (2001) 30231–30244.
[13] A. Bailly, H. Yang, E. Martinoia, et al., Plant lessons: exploring ABCB functionality through structural modeling, Front. Plant Sci. 2 (2011) 1–16.
[14] F.L. Theodoulou, Plant ABC transporters, Biochim. Biophys. Acta 1465 (2000) 79–103.
[15] M. Geisler, A.S. Murphy, The ABC of auxin transport: the role of p-glycoproteins in plant development, FEBS Lett. 580 (2006) 1094–1102.
[16] D. Santelia, V. Vincenzetti, E. Azzarello, et al., MDR-like ABC transporter AtPGP4 is involved in auxin-mediated lateral root and root hair development, FEBS Lett. 579 (2005) 5399–5406.
[17] A. Bailly, V. Sovero, V. Vincenzetti, et al., Modulation of P-glycoproteins by auxin transport inhibitors is mediated by interaction with immunophilins, J. Biol. Chem. 283 (2008) 21817–21826.
[18] B. Wang, A. Bailly, M. Zwiewka, et al., *Arabidopsis* TWISTED DWARF1 functionally interacts with auxin exporter ABCB1 on the root plasma membrane, Plant Cell 25 (2013) 202–214.
[19] M. Geisler, J.J. Blakeslee, R. Bouchard, et al., Cellular efflux of auxin catalyzed by the *Arabidopsis* MDR/PGP transporter *AtPGP1*, Plant J. 44 (2005) 179–194.
[20] M. Sidler, P. Hassa, S. Hasan, et al., Involvement of an ABC transporter in a developmental pathway regulating hypocotyl cell elongation in the light, Plant Cell 10 (1998) 1623–1636.
[21] B. Noh, A.S. Murphy, E.P. Spalding, Multidrug resistance–like genes of *Arabidopsis* required for auxin transport and auxin-mediated development, Plant Cell 13 (2001) 2441–2454.
[22] G.K. Muday, A.S. Murphy, An emerging model of auxin transport regulation, Plant Cell 14 (2002) 293–299.
[23] D.S. Multani, S.P. Briggs, M.A. Chamberlin, et al., Loss of an MDR transporter in compact stalks of maize *br2* and sorghum *dw3* mutants, Science 302 (2003) 81–84.
[24] A.S. Knöller, J.J. Blakeslee, E.L. Richards, et al., Brachytic2/ZmABCB1 functions in IAA export from intercalary meristems, J. Exp. Bot. 61 (2010) 3689–3696.
[25] R. Lin, H. Wang, Two homologous ATP-binding cassette transporter proteins, *AtMDR1* and *AtPGP1*, regulate *Arabidopsis* photomorphogenesis and root development by mediating polar auxin transport, Plant Physiol. 138 (2005) 949–964.
[26] A. Murphy, W.A. Peer, L. Taiz, Regulation of auxin transport by aminopeptidases and endogenous flavonoids, Planta 211 (2000) 315–324.
[27] P.J. Krysan, J.C. Young, M.R. Sussman, T-DNA as an insertional mutagen in *Arabidopsis*, Plant Cell 11 (1999) 2283–2290.